

Lipoproteins Containing the Truncated Apolipoprotein, Apo B-89, Are Cleared from Human Plasma More Rapidly Than Apo B-100-containing Lipoproteins In Vivo

Klaus G. Parhofer, P. Hugh R. Barrett,* Dennis M. Bier,† and Gustav Schonfeld

Division of Atherosclerosis and Lipid Research and †Resource for Biomedical Mass Spectrometry, Department of Internal Medicine, Washington University School of Medicine, 4566 Scott Avenue, Box 8046, St. Louis, Missouri 63110; and *Resource Facility for Kinetic Analysis, Center for Bioengineering, University of Washington, Seattle, Washington 98195

Abstract

We have reported previously on two truncations of apolipoprotein B (apo B-40 and apo B-89) in a kindred with hypobetalipoproteinemia. Premature stop codons were found to be responsible for both apo B-40 and apo B-89, but the physiologic mechanisms accounting for the reduced plasma concentrations of these proteins have not been determined in vivo. This study investigates the metabolism of apo B-89 in two subjects heterozygous for apo B-89/apo B-100 and in one apo B-40/apo B-89 compound heterozygote. In both heterozygotes total apo B concentration is ~ 30% of normal and apo B-89 is present in lower concentrations in plasma than apo B-100. After the administration of [1-¹³C]leucine as a primed constant infusion over 8 h, ¹³C enrichments of plasma leucine as well as enrichments of VLDL-, IDL-, and LDL-apo B-89 leucine and VLDL-, IDL-, and LDL-apo B-100 leucine were measured over 110 h. Enrichment values were subsequently converted to tracer/tracee ratios and a multicompartmental model was used to estimate metabolic parameters. In both apo B-89/apo B-100 heterozygotes apo B-89 and apo B-100 were produced at similar rates. Respective transport rates of apo B-89 and apo B-100 for subject 1 were 2.13±0.18 and 2.56±0.13 mg·kg⁻¹·d⁻¹, and for subject 2, 6.59±0.18 and 8.23±0.39 mg·kg⁻¹·d⁻¹. However, fractional catabolic rates of VLDL, IDL, and LDL particles containing apo B-89 were 1.4–3 times higher than the rates for corresponding apo B-100-containing particles. Metabolic parameters of apo B-89 in the apo B-40/apo B-89 compound heterozygote compared favorably with those established for apo B-89 in apo B-89/apo B-100 heterozygotes. Thus, the enhanced catabolism of VLDL, IDL, and LDL particles containing the truncated apolipoprotein is responsible for the relatively low levels of apo B-89 seen in these subjects. (*J. Clin. Invest.* 1992; 89:1931–1937.) Key words: in vivo kinetics • lipoprotein metabolism • multicompartmental model • truncated apolipoprotein B

Introduction

Apolipoprotein B, a major protein associated with several lipoproteins in plasma, normally exists in two forms, apo B-100

Address correspondence and reprint requests to Dr. Gustav Schonfeld, Division of Atherosclerosis and Lipid Research, Washington University School of Medicine, 4566 Scott Ave., Box 8046, St. Louis, MO 63111.

Received for publication 23 October 1991 and in revised form 9 January 1992.

J. Clin. Invest.

© The American Society for Clinical Investigation, Inc.

0021-9738/92/06/1931/07 \$2.00

Volume 89, June 1992, 1931–1937

and apo B-48. In humans, apo B-100, consisting of 4536 amino acid residues, is synthesized in liver and is present in VLDL, IDL, and LDL, and apo B-48, consisting of 2152 residues (the NH₂-terminus 48% of apo B-100), is found in chylomicrons and chylomicron remnants (1). In addition, several unusual inherited truncations of apo B have been described in subjects with hypobetalipoproteinemia (1–5). We have reported previously on a kindred with hypobetalipoproteinemia and two different truncations of apolipoprotein B (apo B): apo B-40 and apo B-89 (4, 5). All simple heterozygous (apo B-89/apo B-100 or apo B-40/apo B-100) and compound heterozygous (apo B-40/apo B-89) members of this kindred have plasma cholesterol levels below the 10th and 5th percentiles, respectively. In apo B-89/apo B-100 heterozygotes total apo B concentrations are ~ 30% of normal and apo B-89 is present at lower concentrations than apo B-100 in all classes of apo B-containing lipoproteins. Mutations of the apo B gene producing two different premature stop codons are responsible for the apo B-89 and apo B-40 truncations (5), but the physiologic mechanisms accounting for the reduced plasma concentrations of either apo B-40 or apo B-89 containing lipoproteins have not been defined. While apo B-40 is found primarily in the HDL fraction, the density distribution of apo B-89 resembles that of apo B-100 (4). In apo B-89/apo B-100 heterozygotes the two apolipoproteins are known to exist on distinct particles, e.g., apo B-100 LDL and apo B-89 LDL (4, 6). The fact that both apo B-89 and apo B-100 are found in the VLDL, IDL, and LDL density classes implies that both proteins are metabolized via similar pathways. Thus, the low levels of apo B-89 containing lipoproteins in these subjects are probably due to quantitative differences in their production (transport), conversion, or removal rates.

This communication addresses the metabolism of VLDL, IDL, and LDL-apo B-89 in three affected individuals. Apo B metabolism was studied in two apo B-89/apo B-100 heterozygotes and in one apo B-40/apo B-89 compound heterozygote using [1-¹³C]leucine as the endogenously incorporated tracer. Metabolic parameters for apo B-89 and apo B-100 were estimated by multicompartmental modeling. The data indicate that apo B-89 and apo B-100 are produced at approximately equal rates, but apo B-89 containing particles are cleared more rapidly than their apo B-100 containing counterparts.

Methods

Subjects. Two heterozygotes (phenotype apo B-89/apo B-100) and one compound heterozygote (phenotype apo B-40/apo B-89) participated in the study after giving informed consent to the study protocol approved by the Human Studies Committee of Washington University, St. Louis, MO. The clinical characteristics of the subjects are shown in Table I. All subjects were healthy and taking no medications. The subjects did not change their regular diet 10 d before or during the infusion study, or throughout the 110-h study period.

Table 1. Clinical Characteristics of Study Subjects

Subject	Sex	Age yr	Weight kg	BMI kg · m ⁻²	Chol mmol · liter ⁻¹	TG mmol · liter ⁻¹	APO B phenotype
1	male	45	72.1	24.9	3.00	0.64	apo B-89/apo B-100
2	male	20	76.2	27.0	2.56	0.50	apo B-89/apo B-100
3	female	55	71.6	28.0	1.86	0.40	apo B-40/apo B-89

Subject 1 is the father of subject 2. BMI, body-mass-index; Chol, plasma cholesterol; TG, plasma triglycerides.

Materials. [¹³C]leucine was obtained from MSD Isotopes (Montreal, Canada). Isotopic purity was 99%. For use the tracer was dissolved in saline, sterile filtered (0.22 μm; Millipore Corp., Milford, MA), and tested for pyrogens (Scientific Associates Inc., St. Louis, MO). Triethylamine was obtained from Sigma Chemical Co. (St. Louis, MO), ethylacetate from EM Science (Cherry Hill, NJ), and 3.5 N HBr in propanol from Alltech Associates Inc. (Deerfield, IL). Polyacrylamide/bis solutions were prepared from a stock solution (Acryl/bis 37.5:1; Amresco, Solon, OH). All other chemicals were obtained from Fisher Scientific (Fair Lawn, NJ). The cation exchange resin (AG50W-X8; Bio-Rad Laboratories, Richmond, CA) was used in columns (Whale Scientific, Commerce City, CO) for the isolation of amino acids.

Study protocol. After fasting for 10 h, the subjects were admitted to the General Clinical Research Center at 6:00 P.M. An intravenous line was placed in the cubital vein of each arm. One line served for infusion of tracer and the other for blood sampling. At 8:00 P.M., a primed constant infusion was started, consisting of a bolus of [¹³C]leucine (0.85 mg · kg⁻¹), immediately followed by an 8-h constant infusion (at 0.85 mg · kg⁻¹ · hr⁻¹). After the infusion was stopped the subjects remained fasting for another 8 h. 42 samples of plasma were drawn for assays of amino acid enrichment (every 5 min during the first hour, and thereafter every 15 min, later, half hourly and hourly, and finally daily up to 110 h). 32 samples were drawn for VLDL-, IDL-, LDL-apo B leucine enrichment (every 10 min during the first hour, thereafter every 15 min, later, half-hourly, hourly, and finally every other day up to 110 h). Aliquots for determination of VLDL-, IDL-, and LDL-apo B pool sizes were drawn on five occasions during the course of the study. Plasma samples were processed immediately for isolation of lipoproteins, and aliquots were stored at -70°C until analysis.

Analytical methods

Isolation of lipoproteins. VLDL ($d < 1.006 \text{ g} \cdot \text{ml}^{-1}$), IDL ($d 1.006\text{--}1.019 \text{ g} \cdot \text{ml}^{-1}$), and LDL ($d 1.019\text{--}1.063 \text{ g} \cdot \text{ml}^{-1}$) were isolated by sequential ultracentrifugation (7) from 4 ml of plasma using a rotor (50.4 Tl; Beckman Instruments Inc., Palo Alto, CA).

Preparation of apo B and isolation of amino acids. Apo B-89 and apo B-100 were separated by polyacrylamide gel (3–6%) electrophoresis (8) at each time point from each lipoprotein fraction. Aliquots corresponding to 50–100 μg of total protein were applied per lane. Coomassie blue-stained bands of apo B-89 and apo B-100 were excised and hydrolyzed in 12 N HCl for 16 h at 110°C. Amino acids were isolated from the hydrolyzed gel pieces or from 0.3 ml plasma by cation exchange chromatography (9).

Determination of enrichment and calculation of tracer/tracee ratios. Amino acids obtained from the plasma samples or from the hydrolyzed apo B gel bands were derivatized to *n*-acetyl-*n*-propanol-esters (9). Enrichments were determined by gas chromatography-mass spectrometry using 1.5 m × 2.0 mm glass columns (Supelco Inc., Bellefonte, CA) packed with Amino Acid Packing (Alltech Associates Inc.) coupled to a Finnigan 3,300 quadropole mass spectrometer (10). Isotope ratios were calculated from the observed ion current ratio (*m/z* 217/216) using a standard curve. Enrichments were calculated using the method of Cobelli et al. (11). These values were subsequently converted to tracer/

tracee ratios (11). Data in this format are analogous to specific radioactivity in radiotracer experiments.

Lipids and apo B. Plasma lipids were measured by commercially available tests (Wako Chemicals, Richmond, VA). Apo B levels were measured in VLDL, IDL, and LDL fractions by radioimmunoassay (12) and concentrations were confirmed by protein assays (13). The values for apo B concentration measured with the radioimmunoassay did not differ by more than 20% from values estimated from the protein assay, assuming that ~40% of VLDL protein, 70% of IDL protein, and 90% of LDL protein represented apo B. Separation of apo B-89 from apo B-100 was achieved using 3–6% gradient SDS-polyacrylamide gels stained with Coomassie Blue. The protein bands corresponding to apo B-100 and apo B-89 were scanned by laser densitometry. Based on the assumption that both forms of apo B have the same chromogenicity, pool sizes of apo B-89 and apo B-100 were estimated by scanning three to five samples from different time points in each lipoprotein fraction and averaging ratios.

Model for apo B metabolism and calculation of parameters. A simple multicompartmental model (Fig. 1) was used to describe VLDL-, IDL-, and LDL-apo B leucine tracer/tracee ratios. In multicompartmental modeling, each compartment or pool represents a group of kinetically homogenous particles. In this study the CONSAM/SAAM (14) programs were used to fit the model to the observed tracer data. These programs use a weighted least squares approach to find the best possible fit. Metabolic parameters are subsequently derived from this best fit. This model is derived from previously published models (15–18) and has been shown to describe apo B metabolism in four normolipidemic controls (19) who had total plasma cholesterol levels between the 5th and 50th percentile of age-, sex-, and race-matched controls. The model consists of a precursor compartment (compartment 1) and an intracellular delay compartment accounting for the synthesis of apo B and the assembly of lipoproteins (compartment 2). Compartments 11 and 12 are used to account for the kinetics of the VLDL-apo B fraction and represent a minimal delipidation chain. Although only one VLDL sample is obtained at each time point, the two-compartment VLDL model is required to fit the VLDL tracer data. Compartment 11 represents a rapidly turning-over pool of VLDL particles and compartment 12 represents those VLDL particles that turn over more slowly. IDL-apo B (compartment 21) can be derived from either of the two VLDL compartments. LDL-apo B (compartment 31) is derived from the IDL fraction (compartment 21) or directly from VLDL compartment 11 through a shunt pathway. It is assumed that plasma leucine (compartment 1) is the source of the leucine that is incorporated into apo B. Plasma leucine tracer/tracee ratios were described by a triexponential function (described in detail in reference 19) that was used as a forcing function (20) in the model. It is further assumed that all apo B enters the plasma via compartment 11, thus transport rates through compartment 11 correspond to total apo B production. After fitting the model to the observed data, fractional catabolic rates (FCR)¹ and conversion rates were determined for apo B-89 and apo B-100. The FCR of VLDL-apo B is the weighted average (related to mass distribu-

1. Abbreviation used in this paper: FCR, fractional catabolic rate.

tion) of the FCR's of pools 11 and 12. The FCR of each VLDL pool is the sum of individual rate constants (for compartment 11, rate constants relating to the following metabolic pathways: 11 → 12, 11 → 21, 11 → 31, and 11 → out; for compartment 12, rate constants relating to 12 → 21 and 12 → out). The FCR of IDL-apo B corresponds to the sum of individual rate constants of compartment 21 (21 → out and 21 → 31). The FCR of LDL-apo B corresponds to the rate of irreversible loss from compartment 31 (31 → out). The only difference from the previously published model (19) is that a direct loss from compartment 11 (11 → out) was required to fit the observed tracer/tracee ratios of VLDL-apo B-89. Because of the low mass of IDL-apo B-89 in subject 2, tracer/tracee ratios could not be determined. To fit the model to this subject's apo B-89 data, it was assumed that all IDL was converted to LDL (thus, that the flux 21 → out was zero). Furthermore, the FCR of the IDL compartment was free to adjust to provide the delay necessary to fit the LDL data. In this manuscript, the terms transport rate and production rate are used synonymously, as are FCR and fractional turnover rate. The term rate constant refers to the fractional turnover rate of a pool related to a specific pathway (e.g., the fraction of compartment 11 that is converted to compartment 12 per day).

Results

Plasma concentrations of VLDL-, IDL- and LDL-apo B are presented for each subject in Table II. These values represent means of five separate samples taken during the period of fast-

ing. Apo B concentrations remained constant in all lipoprotein fractions, during this period, indicating that each subject remained in a steady state during the course of the study. In all three patients the concentrations of apo B were markedly lower in all lipoprotein fractions compared with values for normolipidemic subjects, and the concentration of apo B-89 was consistently lower than that of apo B-100. In the apo B-89/apo B-100 heterozygotes, the ratio of apo B-89 to apo B-100 decreased with increasing lipoprotein density, i.e., in VLDL, ~ 37% of apo B was apo B-89, while apo B-89 represented only 15% of apo B in LDL. In the compound heterozygote (apo B-40/apo B-89) almost all apo B in VLDL, IDL, and LDL was apo B-89.

Plasma leucine tracer/tracee ratios from a representative study (subject 1) are shown in Fig. 2. After the bolus injection, the first sample at 5 min showed the peak tracer/tracee ratio followed by a rapid fall over the subsequent 30-min period. Thereafter, there was a relatively constant tracer/tracee ratio over 8 h due to the infusion, followed by a rapid fall when the infusion was stopped. The features of the plasma amino acid tracer/tracee ratio curves were very similar in all three subjects. Plasma leucine tracer/tracee ratio curves were fitted with triexponential functions (19). These functions were subsequently used to define the forcing functions used in the multicompartmental model.

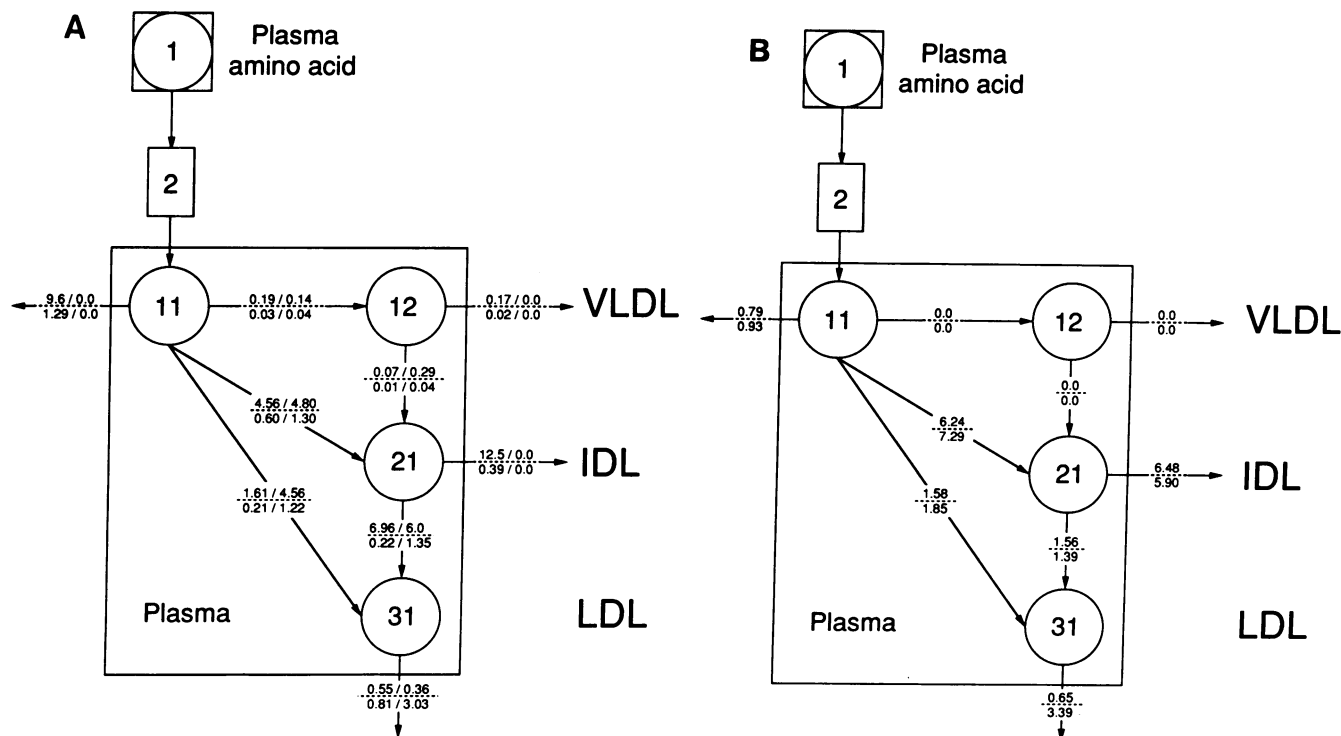


Figure 1. Multicompartmental model for apo B metabolism: (compartment 1) plasma leucine tracer/tracee ratio (forcing function); (compartment 2) delay compartment (synthesis of apo B and secretion of VLDL particles); (compartments 11 and 12) plasma VLDL-apo B; (compartment 21) plasma IDL-apo B; (compartment 31) plasma LDL-apo B. All apo B enters the plasma as VLDL-apo B via compartment 11. Apo B in this rapidly turning-over compartment has one of the following fates: conversion to another VLDL compartment (compartment 12), conversion to IDL-apo B (compartment 21), shunting to LDL-apo B (compartment 31), or removal from plasma. The values above the dotted lines represent transport rates ($\text{mg} \cdot \text{kg}^{-1} \cdot \text{d}^{-1}$) along individual metabolic pathways. In A (subject 1), values to the left of the slash correspond to kinetic parameters for apo B-89 and values to the right of the slash to parameters for apo B-100, i.e., apo B-89/apo B-100. In B (subject 3), parameter values refer to apo B-89. The FCR's presented in Table III and the transport rates presented in Table IV can be calculated from the indicated rate constants as outlined in Methods. As calculated by the model, in subject 1 52% of VLDL-apo B-89 and 62% of VLDL-apo B-100 are in compartment 11, and the rest are in compartment 12; in subject 3 all VLDL-apo B-89 is in compartment 11.

Table II. Apo B Pool Sizes in Different Lipoprotein Fractions

Subject	VLDL-apo B		IDL-apo B		LDL-apo B	
	Concentration	Apo B-89	Concentration	Apo B-89	Concentration	Apo B-89
	$mg \cdot dl^{-1}$	%	$mg \cdot dl^{-1}$	%	$mg \cdot dl^{-1}$	%
1	1.5±0.2	38	0.77±0.11	19	27.2±1.9	15
2	2.4±0.5	35	1.00±0.31	23	22.2±2.2	14
3	2.6±0.4	>90	1.72±0.28	>95	11.5±1.1	>95

Apo B concentrations represent mean values and standard deviations from five measurements.

Figs. 3 and 4 show VLDL (A) and LDL (B) apo B leucine tracer/tracee ratios in the two apo B-89/apo B-100 heterozygotes (subjects 1 and 2). The symbols represent observed values while the lines represent the best fit of the multicompartmental model (Fig. 1) to the tracer data. As can be seen in Figs. 3 and 4, there is good agreement between the model-derived fits and the observed apo B-89 and apo B-100 tracer data. Both the upward and the downward slopes of the tracer/tracee ratio curves for VLDL-apo B-89 were steeper than the analogous slopes for VLDL-apo B-100, and "plateau" values were reached earlier for the tracer/tracee ratios of the truncated protein (A). In the LDL fractions (B) the slopes of the tracer/tracee ratio curves were also steeper for the apo B-89 than for apo B-100-containing particles, and the tracer/tracee ratios in LDL-apo B-89 curves peaked at higher values than in the LDL-apo B-100 curves. Similar data were obtained for the IDL of subject 1 (not shown). The apo B tracer/tracee ratio curves in both apo B-89/apo B-100 heterozygotes (Figs. 3 and 4) showed similar characteristics. The differences in upward and downward slopes in all three lipoprotein fractions, together with the earlier "plateau" in VLDL and the higher peaks in LDL, represent increased rates of appearance and disappearance of labeled apo B-89 compared with the labeled apo B-100 containing lipoproteins.

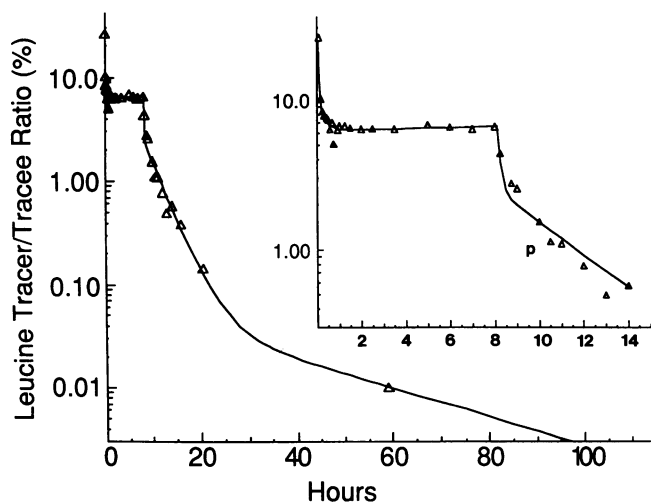


Figure 2. Plasma leucine tracer/tracee ratio after a primed constant infusion of $[1-^{13}C]$ leucine in subject 1. A triexponential function was computer fitted (line) to observed plasma leucine tracer/tracee ratios (symbols) as described previously (19). This function was subsequently used as a forcing function to describe the input of the tracer for the modeling process.

While the qualitative differences between the kinetics of apo B-89 and apo B-100 can be appreciated from the figures directly, multicompartmental modeling is necessary to quantify these differences (Fig. 1). The lag time before the appear-

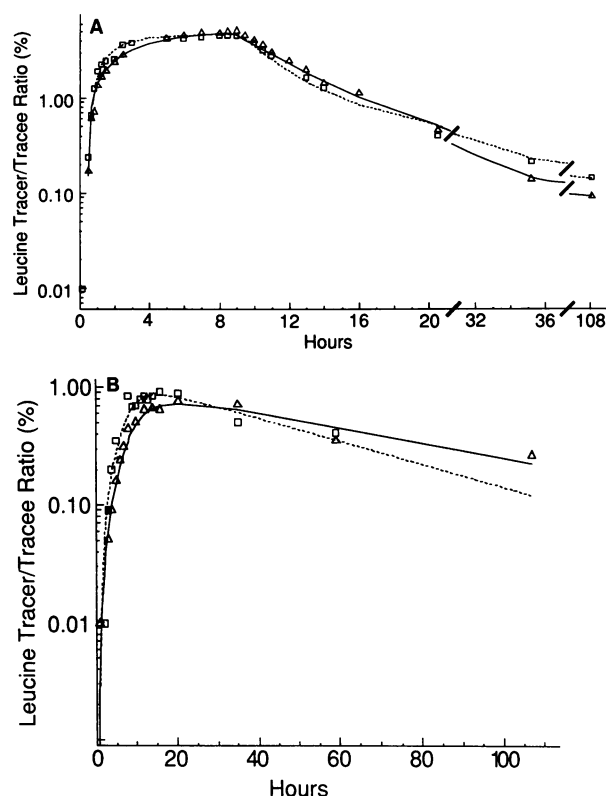


Figure 3. Apo B-89 and apo B-100 leucine tracer/tracee ratios after a primed constant infusion of $[1-^{13}C]$ leucine over 8 h in an apo B-89/apo B-100 heterozygote (subject 1). A shows the data in the VLDL fraction and B in the LDL fraction. For both fractions observed, values are given in symbols and model predicted values are given as lines. Data for apo B-89 are squares \square and the dotted line, and for apo B-100, triangles (Δ) and the solid line. Note the following: (a) the upward and downward slopes of the tracer/tracee ratio curves for apo B-89 are steeper than those of the apo B-100 curves for both the VLDL and LDL fractions; (b) the tracer/tracee ratio curves reach a "plateau" at an earlier time point for VLDL-apo B-89 compared with VLDL-apo B-100; and (c) the tracer/tracee ratio of LDL-apo B-89 reaches a higher level than that of LDL-apo B-100. These features are the expression of the increased FCR of apo B-89 compared with apo B-100.

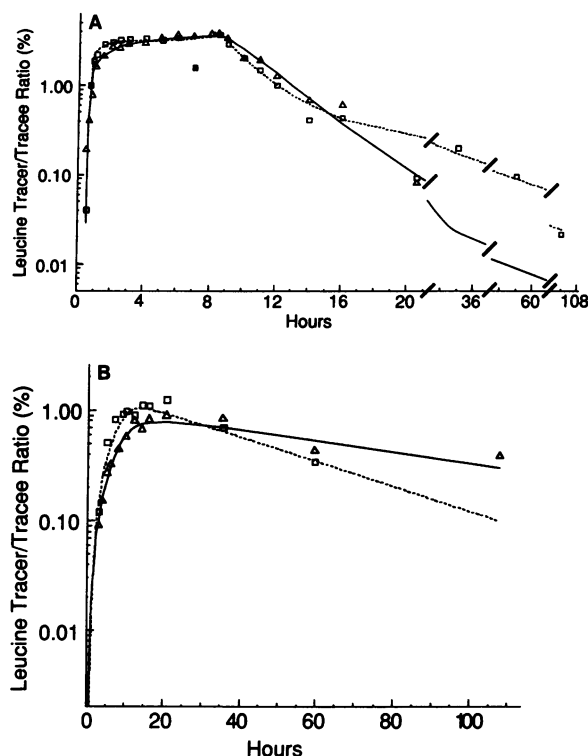


Figure 4. Apo B-89 and apo B-100 leucine tracer/tracee ratios in an apo B-89/apo B-100 heterozygote (subject 2). *A* shows the data in the VLDL fraction and *B* in the LDL fraction. For both fractions observed values (symbols) and model predicted values (lines) for apo B-89 (\square , dotted line) and apo B-100 (Δ , solid line) are shown. For more detailed comment please see legend to Fig. 3.

ance of labeled apo B-89 and apo B-100 in the VLDL fraction was ~ 0.5 h for both proteins. Tables III and IV show metabolic parameters for apo B-89 and apo B-100 derived by multicompartmental modeling. Of particular interest are the parameters derived from the apo B-89/apo B-100 heterozygotes (subjects 1 and 2) in whom the metabolism of the truncated apo B can be compared with that of the normal apo B-100 under identical conditions. The FCR's of apo B-89 were 1.4–3 times higher than those of apo B-100 in all lipoprotein fractions. As described in Methods, the multicompartmental model used for the analysis of apo B tracer/tracee ratio data assumed that all apo B entered plasma as VLDL. VLDL-apo B transport rates therefore reflect total apo B production rates in each subject. In

the apo B-89/apo B-100 heterozygotes, VLDL-apo B transport rates were similar for apo B-89 and apo B-100 (Table IV). The increased FCR of apo B-89 reflects an enhanced irreversible loss of particles from each lipoprotein fraction rather than an increased conversion of VLDL to LDL. Thus, less apo B-89 ultimately reached the LDL fraction as compared with the apo B-100. The greater selective losses of apo B-89 from VLDL are also evident from the fact that with increasing particle density the ratio of apo B-89 mass to apo B-100 mass decreased (Table II). In Fig. 1 all rate constants as well as all transport rates are presented for one of the apo B-89/apo B-100 heterozygotes (subject 1, *A*), as well as for the apo B-40/apo B-89 compound heterozygote (subject 3, *B*). Note that in the apo B-89/apo B-100 heterozygote, the rate constants of all removal pathways are higher for apo B-89 than for apo B-100.

In the two apo B-89/apo B-100 heterozygotes it was possible to compare the metabolism of apo B-89 lipoproteins with that of apo B-100 lipoproteins. Apo B-100 lipoproteins serving as "internal controls" for the metabolism of "normal" apo B containing particles. No such references were available for comparison in the compound heterozygote; however, the metabolic parameters for apo B-89 in this subject were similar to those estimated for apo B-89 in the apo B-89/apo B-100 heterozygotes (Tables III and IV). Fig. 5 shows the tracer/tracee ratios for VLDL-, IDL-, and LDL-apo B-89 in the compound heterozygote (apo B-40/apo B-89). It can also be seen that in this subject there is good agreement between the multicompartmental fit and the observed data.

Discussion

This is the first report of in vivo kinetics of any truncated apolipoprotein in human subjects using stable isotopically labeled amino acids as endogenous tracers. Our studies show that in apo B-89/apo B-100 heterozygotes, the low levels of apo B-89 relative to apo B-100 are due to increased FCR's of lipoproteins containing the truncated protein, while rates of production of apo B-89 are similar to those for apo B-100. By contrast, the FCR's of the truncated apolipoproteins are consistently higher in each lipoprotein fraction. The enhanced FCR's result from increased removal rates for each density class rather than increased conversion rates of lower to higher density lipoproteins, i.e., compared with apo B-100, a greater proportion of apo B-89 is irreversibly removed from the VLDL and IDL compartments before being converted. The FCR of LDL is also higher for apo B-89 than for apo B-100 containing particles. The differences seen in the production rates between subjects 1

Table III. Fractional Catabolic Rates of Apo B-89 and Apo B-100 in VLDL, IDL, and LDL

Subject	VLDL		IDL		LDL	
	Apo B-89 FCR	Apo B-100 FCR	Apo B-89 FCR	Apo B-100 FCR	Apo B-89 FCR	Apo B-100 FCR
	d^{-1}					
1	8.4 \pm 0.7	6.0 \pm 0.2	19.4 \pm 1.9	6.0 \pm 1.9	0.55 \pm 0.05	0.36 \pm 0.05
2	17.5 \pm 0.5	11.8 \pm 0.5	*	5.0 \pm 0.5	0.67 \pm 0.07	0.29 \pm 0.05
3	8.6 \pm 0.7	—	8.1 \pm 0.5	—	0.65 \pm 0.05	—

FCR, fractional catabolic rate. Values represent best estimates \pm SD. * IDL-apo B-89 in subject 2 was present in concentrations too low to quantify [13 C]leucine enrichments with precision.

Table IV. Metabolic Parameters for Apo B-89 and Apo B-100

Subject	Apo B transport (production rate, comp.2 → comp.11)		VLDL-apo B converted to LDL-apo B (comp.11 → ... → comp.31, by all possible pathways*, see model)	
	apo B-89	apo B-100	apo B-89	apo B-100
	<i>mg · kg⁻¹ · d⁻¹</i>		<i>%</i>	
1	2.13±0.18	2.56±0.13	20.3±1.5	100.0±7.0
2	6.59±0.18	8.23±0.39	16.1±1.6	69.8±4.5
3	10.10±0.41	—	32.2±2.5	—

* Includes conversion via the classical VLDL-IDL-LDL pathway, as well as direct shunting, see Fig. 1. Values represent best estimates ± SD.

and 2 (father and son) may be related to the age of the subjects. Despite differences between father and son in absolute terms, the apo B-89/apo B-100 ratios for the kinetic parameters are similar. Apo B-40 metabolism was not studied in the compound heterozygote (3) because of the extremely low plasma levels of this apolipoprotein.

These results are in accord with our earlier studies showing that apo B-89 containing LDL bound to cultured fibroblasts with greater affinity than apo B-100 containing LDL (4), and that the FCR of apo B-89 containing LDL was double that of apo B-100 containing control LDL in rabbits (6). While these cell culture and animal studies demonstrated the different metabolic behavior of apo B-89 containing LDL, the metabolism of VLDL and IDL was not studied. The present in vivo studies demonstrate that not only LDL but all particles containing apo B-89 (VLDL, IDL, and LDL) were cleared from plasma at enhanced rates compared with apo B-100 containing particles. Based on our previous findings (4, 6), these data are consistent with an enhanced removal of the lipoproteins via LDL receptors as the most likely mechanism. Favorable conformational

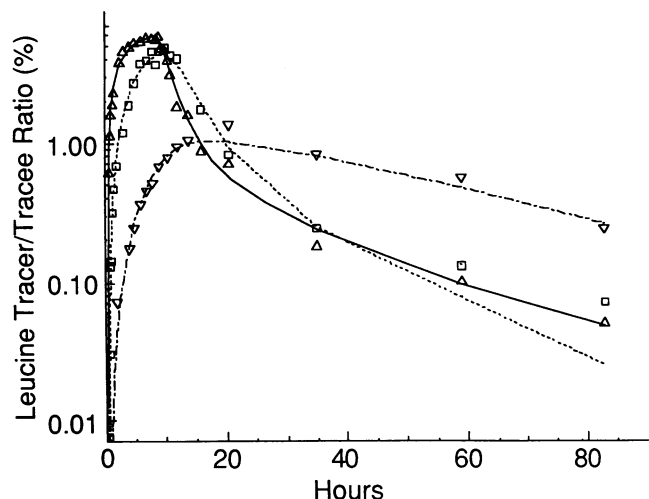


Figure 5. Observed values (symbols) and predicted values (lines) for the VLDL-, IDL-, and LDL-apo B-89 tracer/tracee ratios in the apo B-40/apo B-89 compound heterozygote using the multicompartmental model. VLDL-(Δ , solid line), IDL-(\square , dotted line), and LDL-apo B (∇ , dashed line) leucine tracer/tracee ratios after a primed constant infusion of [$1\text{-}^{13}\text{C}$]leucine are shown.

changes in the LDL receptor recognition region of apo B-89 resulting in an enhanced binding to the receptor could account for this observation. Other factors, however, such as a slightly different apoprotein composition of the lipoproteins containing apo B-89 (e.g., increased apo E content or altered apo E/apo C ratio), a different stability of these particles, or an altered interaction with lipase cannot be excluded. Since the conformation of apo B-100 varies on particles of different sizes (21, 22), and since apo B-89 LDL are smaller than apo B-100 LDL (6), it is possible that the conformational differences are related more to the truncation-induced reduction in LDL size and any resulting changes in the curvature of apo B on the surfaces of the smaller particles, rather than to any conformational changes due to the 11% deletion of the COOH-terminal portion of the protein per se. However, the enhanced catabolism of apo B-89 containing lipoproteins of all density classes, which range widely in size, favors the idea that it is the truncation itself that is responsible for the increased clearance. It should be noted, however, that hypobetalipoproteinemia associated with other truncations of apo B may be mediated through different mechanisms, such as a decreased production rate and/or a different catabolic rate.

It is remarkable that the concentrations of both populations of apo B containing lipoproteins (apo B-89 and apo B-100) are relatively low in the plasmas of simple heterozygotes, raising the question that the metabolism of the apo B-100 particles also could be altered. Because of the wide normal range for metabolic parameters of apo B (18, 19), it is difficult to reach definitive conclusions on this point. We have found the FCR's of control subjects with plasma total cholesterol concentrations ranging between 3.3–4.4 mmol · liter⁻¹ (5–50th percentile for sex, age, and race), to vary between 6.7 and 11.3 d⁻¹ for VLDL-apo B-100, and between 0.19 and 1.10 d⁻¹ for LDL-apo B-100, using the same methodology and an almost identical kinetic model (19). The FCRs for apo B-100 in our heterozygotes were similar to those obtained in our control subjects, suggesting that perhaps LDL-receptor activity is not upregulated in heterozygotes despite their low cholesterol levels. Production rates of apo B-100 for the controls ranged between 8.0 and 23.6 mg · kg⁻¹ · d⁻¹, and total production rates for apo B (apo B-89 plus apo B-100) in our heterozygotes fell at the lower end of this range. Thus, a reduced production rate of total apo B could be contributing to the hypobetalipoproteinemia seen in this kindred, but larger numbers of subjects need to be studied before this can be concluded with statistical certainty.

Two potential weaknesses of this study need to be discussed: (a) the appropriateness of the kinetic model; and (b) the accuracy of the estimated pool sizes. Leucine labeled with radioisotopes (24) or with stable isotopes (19, 25–27) have been used previously to study apolipoprotein metabolism. The model presented here is based on previously published models (15–18), and as demonstrated here, the model we developed for control subjects (19) can also describe the metabolism of our patients with only a slight modification of the model. We do, however, appreciate that this model may not fit tracer data of other apo B truncations, particularly when the metabolic pathways of the truncated apo B are different from those of apo B-100 (e.g., in apo B-40 or apo B-54.8 [2] where LDL receptor recognition regions may be absent). Furthermore, it should be noted that recycling of the tracer might impair the calculation of kinetic parameters. As discussed elsewhere (19), the problem of recycling impacts less upon the estimates of kinetic parameters of

rapidly turning-over particles, i.e., VLDL, IDL, and more upon slowly turning-over particles such as LDL.

Pool sizes of apo B-89 and apo B-100 were estimated on the assumption that both proteins have the same chromogenicity. While it has been shown that apo B-48 differs in this respect from apo B-100 (23), this is unknown for apo B-89. However, the similar molecular size of apo B-100 and apo B-89 makes significant differences unlikely. To the extent that estimated pool sizes are under- or overestimated, calculated production rates could also be in error. In fact, apo B production from the VLDL-IDL-LDL cascade combined with that from the shunt pathway could not account for all the apo B mass in the LDL fraction. As pointed out previously by us (19) and others (24), this most likely reflects errors associated with the determination of pool sizes. While the percentage of apo B unaccounted for in the LDL fraction averaged around 7% in normolipidemic subjects (19), this value was higher in subject 1 (Fig. 1), amounting to $0.38 \text{ mg} \cdot \text{kg}^{-1} \cdot \text{d}^{-1}$ of the total apo B-89 production of $2.13 \text{ mg} \cdot \text{kg}^{-1} \cdot \text{d}^{-1}$. Errors in the determination of the pool sizes are probably greater in these subjects due to their extremely low levels of apo B. However, since calculations of FCR's for apo B-89 and apo B-100 containing lipoprotein fractions are independent of pool sizes, the major conclusions of the study are largely unaffected by any errors that may or may not have been associated with the determination of the pool size.

Studies of heterozygotes carried out under these conditions offer the further advantage that any conclusions concerning the metabolism of a mutant protein (e.g., apo B-89) are largely independent of the kinetic model chosen to calculate the results, because parameters for the mutant protein are compared with those for the "wild type" protein (e.g., apo B-100) obtained in the same subject, at the same time, under identical conditions. Thus, the normal protein serves as an "internal control" for the mutant form. It may be anticipated that a similar experimental format could be usefully applied to a variety of other mutations of plasma proteins in humans.

In summary, metabolic parameters for a truncated apolipoprotein have been established in affected individuals for the first time. Apo B-89 is produced at a similar rate as apo B-100, but has a higher FCR in each lipoprotein fraction. Thus, an enhanced catabolism of VLDL, IDL, and LDL containing the truncated apolipoprotein is responsible for the relatively low concentration of apo B-89 seen in these subjects.

Acknowledgments

We thank Angela Crisci and Julie Dunn for expert technical help, Kathy Garlock for patient recruitment, and the staff of the General Clinical Research Center at Washington University for help in the human studies.

This work was supported by grants from the National Institutes of Health (RR-02176, HL-30086, HL-15308, RR-00954, and HD-20805). Klaus Parhofer is a Fellow of the American Heart Association, Missouri Affiliate. Hugh Barrett is a recipient of a travel grant of the National Heart Foundation of Australia.

References

1. Young, S. G. 1989. Recent progress in understanding apolipoprotein B. *Circulation*. 82:1574-1594.
2. Wagner, R. D., E. S. Krul, J. J. Tang, K. G. Parhofer, K. Garlock, P. Talmud, and G. Schonfeld. 1991. Apo B-54.8, a truncated apolipoprotein found primarily in VLDL is associated with a nonsense mutation in the apoB gene and hypobetalipoproteinemia. *J. Lipid Res.* 32:1001-1011.
3. Welty, F. K., S. T. Hubl, V. R. Pierotti, and S. G. Young. 1991. A truncated species of apolipoprotein B (B67) in a kindred with familial hypobetalipoproteinemia. *J. Clin. Invest.* 87:1748-1754.
4. Krul, E. S., M. Kinoshita, P. Talmud, S. E. Humphries, S. Turner, A. C. Goldberg, E. Boerwinkle, and G. Schonfeld. 1989. Two distinct truncated apolipoprotein B species in a kindred with hypobetalipoproteinemia. *Arteriosclerosis*. 9:856-868.
5. Talmud, P., L. King-Underwood, E. S. Krul, G. Schonfeld, and S. Humphries. 1989. The molecular basis of truncated forms of apolipoprotein B in a kindred with compound heterozygous hypobeta-lipoproteinemia. *J. Lipid Res.* 30:1773-1779.
6. Parhofer, K. G., A. Daugherty, M. Kinoshita, and G. Schonfeld. 1990. Enhanced clearance from plasma of low density lipoproteins containing a truncated apolipoprotein apoB-89. *J. Lipid Res.* 31:2001-2007.
7. Havel, R. J., H. A. Eder, and J. H. Bragdon. 1955. The distribution and chemical composition of ultracentrifugally separated lipoproteins in human serum. *J. Clin. Invest.* 34:1345-1353.
8. Laemmli, U. K. 1970. Cleavage of structural proteins during the assembly of the head of bacteriophage T4. *Nature (Lond.)* 227:680-685.
9. Adams, R. F. 1974. Determination of amino acid profiles in biological samples by gas chromatography. *J. Chromatogr.* 95:189-212.
10. Matthews, D. E., E. Ben-Galim, and D. M. Bier. 1979. Determination of stable isotopic enrichment in individual plasma amino acids by chemical ionization mass spectrometry. *Anal. Chem.* 51:80-84.
11. Cobelli, C., G. Toffolo, D. M. Bier, and R. Nosadini. 1987. Models to interpret kinetic data in stable isotope tracer studies. *Am. J. Physiol.* 253:E551-E564.
12. Schonfeld, G., R. S. Lees, P. K. George, and B. Pfeleger. 1974. Assay of total plasma apolipoprotein B concentration in human subjects. *J. Clin. Invest.* 53:1458-1467.
13. Lowry, O. H., N. J. Rosebrough, A. L. Farr, and R. J. Randall. 1951. Protein measurement with the Folin phenol reagent. *J. Biol. Chem.* 193:265-275.
14. Berman, M. 1978. SAAM Manual. DHEW Publ. No-NIH. 78-180:1-196.
15. Berman, M., M. Hall, R. I. Levy, S. Eisenberg, D. W. Bilheimer, R. D. Phair, and R. H. Goebel. 1978. Metabolism of apoB and apoC lipoproteins in man: kinetic studies in normal and hyperlipoproteinemic subjects. *J. Lipid Res.* 19:38-56.
16. Packard, C. J., A. Munro, A. R. Lorimer, A. M. Gotto, and J. Shepherd. 1984. Metabolism of apolipoprotein B in large triglyceride-rich very low density lipoproteins of normal and hypertriglyceridemic subjects. *J. Clin. Invest.* 74:2178-2192.
17. Beltz, W. F., Y. A. Kesaniemi, B. V. Howard, and S. M. Grundy. 1985. Development of an integrated model for analysis of the kinetics of apolipoprotein B in plasma very low density lipoproteins, intermediate density lipoproteins, and low density lipoproteins. *J. Clin. Invest.* 76:575-585.
18. Kesaniemi, Y. A., G. L. Vega, and S. M. Grundy. 1982. Kinetics of apolipoprotein B in normal and hyperlipidemic man: review of current data. In *Lipoprotein Kinetics and Modeling*, M. Berman, S. M. Grundy, and B. V. Howard, editors. Academic Press, New York. pp. 181-205.
19. Parhofer, K. G., P. H. Barrett, D. M. Bier, and G. Schonfeld. 1991. Determination of kinetic parameters of apolipoprotein B metabolism using amino acids labeled with stable isotopes. *J. Lipid Res.* 32:1001-1011.
20. Berman, M. 1978. A deconvolution scheme. *Math. Biosci.* 40:319-323.
21. Keidar, S., A. C. Goldberg, K. Cook, J. Bateman, and G. Schonfeld. 1989. High carbohydrate-fat free diet modulates epitope expression of LDL-apoB-100 and interaction of LDL with human fibroblasts. *J. Lipid Res.* 30:1331-1339.
22. Keidar, S., A. C. Goldberg, K. Cook, J. Bateman, and G. Schonfeld. 1989. A high carbohydrate-fat free diet alters the proportion of heparin-bound VLDL in plasma and the expression of VLDL-apoB-100 epitopes. *Metab. Clin. Exp.* 39:281-288.
23. Poapst, M., K. Uffelman, and G. Steiner. 1987. The chromogenicity and quantitation of apoB-100 and apoB-48 of human plasma lipoproteins on analytical SDS gel electrophoresis. *Atherosclerosis*. 65:75-88.
24. Beltz, W. F., Y. A. Kesaniemi, N. H. Miller, W. R. Fisher, S. M. Grundy, and L. A. Zech. 1990. Studies on the metabolism of apolipoprotein B in hypertriglyceridemic subjects using simultaneous administration of tritiated leucine and radioiodinated very low density lipoprotein. *J. Lipid Res.* 31:361-374.
25. Cryer, D. R., T. Matsushima, J. B. Marsh, M. Yudkoff, P. M. Coates, and J. A. Cortner. 1986. Direct measurement of apolipoprotein B synthesis in human very low density lipoprotein using stable isotopes and mass spectrometry. *J. Lipid Res.* 27:508-516.
26. Cohn, J. S., D. A. Wagner, S. D. Cohn, J. S. Millar, and E. J. Schaefer. 1990. Measurement of very low density and low density lipoprotein apolipoprotein (apo) B-100 and high density lipoprotein apo AI production in human subjects using deuterated leucine. *J. Clin. Invest.* 85:804-811.
27. Lichtenstein, A. H., J. S. Cohn, D. L. Hachey, J. S. Millar, J. M. Ordovas, and E. J. Schaefer. 1990. Comparison of deuterated leucine, valine, and lysine in the measurement of human apolipoprotein AI and B-100 kinetics. *J. Lipid Res.* 31:1693-1701.